

# Comparative studies between synthetic routes of SiO<sub>2</sub>@Au composite nanoparticles

Lu Zhang<sup>a,b</sup>, Yong-Gang Feng<sup>a</sup>, Li-Ying Wang<sup>a</sup>, Jun-Yan Zhang<sup>b</sup>,  
Meng Chen<sup>a,b,\*</sup>, Dong-Jin Qian<sup>a</sup>

<sup>a</sup> Department of Chemistry and Laboratory of Advanced Materials, Fudan University, 220 Handan Rd., Shanghai 200433, PR China

<sup>b</sup> State Key Laboratory of Solid Lubrication, Lanzhou Institute of Chemical Physics, Chinese Academy of Science, Lanzhou 730000, PR China

Received 7 September 2006; received in revised form 27 October 2006; accepted 4 November 2006

Available online 15 December 2006

## Abstract

We studied two different methods for the deposition of Au nanoparticles (Au NPs) onto the functionalized silica microspheres. One method was to mix the two kinds of particles together and react at room temperature overnight. The other one was to reduce hydrochloroauric acid to Au NPs with sodium citrate in the presence of the functionalized silica microspheres (one for the naked silica microspheres, the other for the Au-attached silica microspheres). We investigated the morphologies of SiO<sub>2</sub>@Au composite nanoparticles synthesized by these two methods, and found that the latter achieved a denser Au coverage on silica microspheres. Furthermore, we studied the effect of the pH values in a wide range, respectively, for the two methods. A possible mechanism was put forward to interpret the formation of SiO<sub>2</sub>@Au composite nanoparticles and the effects of the synthetic routes and pH values on the morphologies and optical properties.

© 2006 Elsevier Ltd. All rights reserved.

**Keywords:** A. Nanostructures; B. Chemical synthesis; C. Electron microscopy

## 1. Introduction

Metal nanoparticles have always been attracting extensive attention due to their unusual electrical [1], optical [2–4], magnetic [5,6] and catalytic [7,8] properties. They exhibit more excellent properties when they are assembled into different structures. So far, a series of nanostructures, such as nanowires [9,10], nanorods [11–13], nanotubes [14–16] nanotriangles [17] and nanoribbons [18] have been successfully synthesized. Properties of these nanoscale materials are dependent not only on the nature of nanoparticles, but on their shape and size as well.

The core-shell nanomaterials, as one of the complex nanostructures, have been widely studied. Inorganic nanoparticles can obtain improved chemical stability and size monodispersity through deposition onto the inert supports in this type of nanostructure. Recently, there are many reports on the deposition of various inorganic nanoparticles onto silica microspheres, including metals [19–21], metal oxides [22–24] and sulfides [25,26]. Au nanoparticles (Au NPs) are widely used metal nanoparticles for the deposition onto silica microspheres. The typical method contains three steps: the

\* Corresponding author at: Department of Chemistry and Laboratory of Advanced Materials, Fudan University, 220 Handan Rd., Shanghai 200433, PR China. Tel.: +86 21 55664181; fax: +86 21 55664192.

E-mail address: [chenmeng@fudan.edu.cn](mailto:chenmeng@fudan.edu.cn) (M. Chen).

synthesis of silica microspheres; the surface functionalization of silica microspheres with silane coupling agents; deposition of Au NPs onto the functionalized silica microspheres by simply mixing the two kinds of particles. Obviously, the three-step method has been widely used for its convenient manipulation. However, the process is tedious, and the Au coverage on silica microspheres is not dense. Halas and co-workers [27] already made a detailed study for the three-step method. They found that the surface functionalization of silica microspheres with different terminal groups had a significant influence on the Au coverage. The hydrophilic groups, such as amino ( $\text{NH}_2$ ) and mercapto ( $\text{SH}$ ) groups promoted the attachment of Au NPs, while the hydrophobic groups, such as methyl ( $\text{CH}_3$ ) and diphenylphosphine ( $\text{PPh}_2$ ) groups could not favor the attachment of Au NPs. They also studied the impact of mixture of organosilanes and mixture of solvents on the coverage and morphologies of the attached Au NPs. People are now making great effort to optimize the reaction conditions of the three-step method and to explore novel methods to improve the Au coverage on silica microspheres. In addition, sonochemical deposition [20], electroless deposition [28] and seeded growth [29] have been successfully used for the deposition of Au NPs onto silica microspheres.

In the present work, we used a simplified method [30] to prepare  $\text{SiO}_2$ @Au core-shell composite nanoparticles, and compared it with the three-step method. Firstly, silica microspheres were functionalized with the silane coupling agent. Secondly, hydrochloroauric acid was reduced to Au NPs with sodium citrate in the presence of the functionalized silica microspheres. By contrast with the general three-step method, the procedure was simplified, the reaction time was remarkably shortened, and the Au coverage on silica microspheres was denser shown by scanning electron microscope (SEM). We also studied, respectively, the influence of the pH values in a wide range on the Au coverage in these two methods. The results indicated that the pH values had significant influence on the Au coverage on silica microspheres.

## 2. Experimental

### 2.1. Reagents

Tetraethoxysilane (TEOS), aminopropyltriethylsilane (APTES), hydrochloroauric acid and sodium citrate were purchased from Shanghai Chemical Reagent Co. Other reagents were of analytical grade. All the chemicals were used without further purification.

### 2.2. Synthesis and functionalization of silica microspheres

Silica microspheres were prepared using the Stober method [31]. Briefly speaking, 2 mL of 28% ammonia hydrate was mixed with 20 mL of absolute ethanol. The solution was stirred overnight after 1 mL of TEOS was added through the syringe dropwise. The produced silica microspheres were centrifuged from the solution and redispersed in ethanol at least three times to remove excess reactants, then dispersed in 20 mL of absolute ethanol.

For the surface functionalization of silica microspheres, 0.1 mL of APTES was added dropwise to 20 mL of the obtained silica colloidal suspension with vigorous stirring after the injection of 0.5 mL of ammonia. The silica microspheres were centrifuged and redispersed in 20 mL of absolute ethanol after stirring for 4 h. The above procedure was repeated twice to make sure the surface functionalization was complete. The final products were centrifuged and redispersed in ethanol at least three times to remove excess reactants, then dispersed in 20 mL of distilled water for further use.

### 2.3. Deposition of Au NPs onto silica microspheres I

In our work, the deposition of Au NPs onto silica microspheres was carried out using three different strategies. In the generally three-step method (Fig. 1), the amino-terminated silica colloidal suspension was simply mixed with the Au hydrosol. The Au hydrosol prepared using the following steps: 5 mL of the aqueous solution of hydrochloroauric acid (10 mM) was diluted to 50 mL with distilled water, and heated to 100 °C in the oil bath under refluxing. Then, 5 mL of the aqueous solution of sodium citrate (38.8 mM) was rapidly injected into the solution. The mixture was allowed to reflux for further 15 min when its color turned deep red. The obtained Au hydrosol was cooled to room temperature without further purification. In the next step, 1 mL of the amino-terminated silica colloidal suspension was added to 10 mL of the Au hydrosol, and the mixture was stirred under room temperature overnight. The final products were centrifuged and redispersed in distilled water for several times, then dispersed in 10 mL of distilled water.

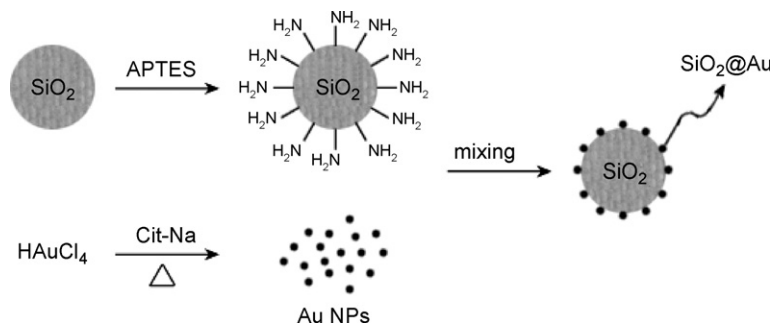


Fig. 1. Schematic illustration of the deposition of Au NPs onto silica microspheres I.

#### 2.4. Deposition of Au NPs onto silica microspheres II

The second strategy was a simplified one (Fig. 2).  $\text{HAuCl}_4$  was reduced to Au NPs with sodium citrate in the presence of the functionalized silica microspheres. In this method, 2.5 mL of hydrochloroauric acid (10 mM) was added to 22.5 mL of the dilute functionalized silica colloidal suspension, and the solution was heated to 100 °C in the oil bath under refluxing. Then, 2.5 mL of sodium citrate (38.8 mM) was rapidly injected into the solution. The mixture was allowed to reflux for further 15 min when its color turned deep red. The obtained products were centrifuged and redispersed in distilled water for several times, then dispersed in 20 mL of distilled water.

#### 2.5. Deposition of Au NPs onto silica microspheres III

The third strategy was derived from the second simplified one (Fig. 3). We first prepared the  $\text{SiO}_2@Au$  composite nanoparticles using the three-step method, and substituted them for the naked functionalized silica microspheres to be mixed with  $\text{HAuCl}_4$  in the aqueous solution. Sodium citrate was rapidly injected to the solution when it was heated to 100 °C under refluxing. The mixture was allowed to reflux for further 15 min. The obtained products were centrifuged and redispersed in distilled water for several times, then dispersed in 20 mL of distilled water.

A series of experiments were designed to explore the effect of the pH values on the Au coverage deposited on silica microspheres. In the three-step method, the pH values of the treatment solutions were adjusted in a wide range prior to stirring overnight. The adjusted pH values included 3.77, 4.65, 5.51, 6.30, 7.79, 9.08, 9.55 and 10.17. In the simplified method, the pH values of the dilute silica colloidal suspensions were adjusted in a wide range prior to addition of  $\text{HAuCl}_4$ . The pH values were adjusted as follows: 3.85, 4.86, 5.38, 7.89 and 8.90. All the pH adjustments were carried out with the aqueous solutions of hydrochloric acid and sodium hydrate.

#### 2.6. Characterization

The UV–vis absorption spectra were taken at room temperature on a UV-3150 spectrophotometer (Shimadzu, Japan) with a variable wavelength between 250 and 700 nm using a glass cuvette with 1-cm optical path. The morphologies of  $\text{SiO}_2@Au$  samples were observed using a Shimadzu SSX-550 scanning electron microscope. The morphologies of Au NPs were observed using a Hitachi H-600 transmission electron microscope (TEM), which was operated at 75 kV with samples deposited onto a 230-mesh copper grid covered with Formvar. Particle size analysis was carried out by manually digitizing the TEM and SEM images with Image Tool, from which the average size and



Fig. 2. Schematic illustration of the deposition of Au NPs onto silica microspheres II.

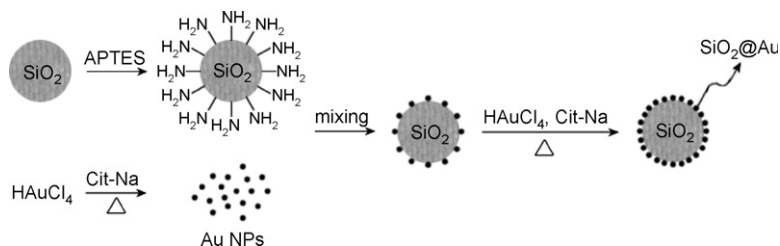


Fig. 3. Schematic illustration of the deposition of Au NPs onto silica microspheres III.

standard deviation of particles were generated. The Au contents of the  $\text{SiO}_2\text{@Au}$  samples were measured using a Z-500 atom absorption spectrometer (AAS).

### 3. Results and discussion

#### 3.1. $\text{SiO}_2\text{@Au}$ composite nanoparticles I

Silica microspheres and the Au hydrosol were prepared, respectively. The naked silica microspheres with smooth surfaces (Fig. 4a) had an average diameter of 227 nm and a narrow size distribution of 9.2% (Fig. 4b). Au NPs were basically spherical as shown in Fig. 4c, which had an average diameter of 14 nm and the size distribution of 13.6% (Fig. 4d). The  $\text{SiO}_2\text{@Au}$  composite nanoparticles was prepared using the general three-step method. The SEM images revealed the morphologies of the  $\text{SiO}_2\text{@Au}$  composite nanoparticles, which showed distinctly that Au NPs were attached to the surfaces of the functionalized silica microspheres (Fig. 5). At lower pH values, sparse Au NPs were distributed on the functionalized silica microspheres (Fig. 5a–d). As the pH values were adjusted to lower levels

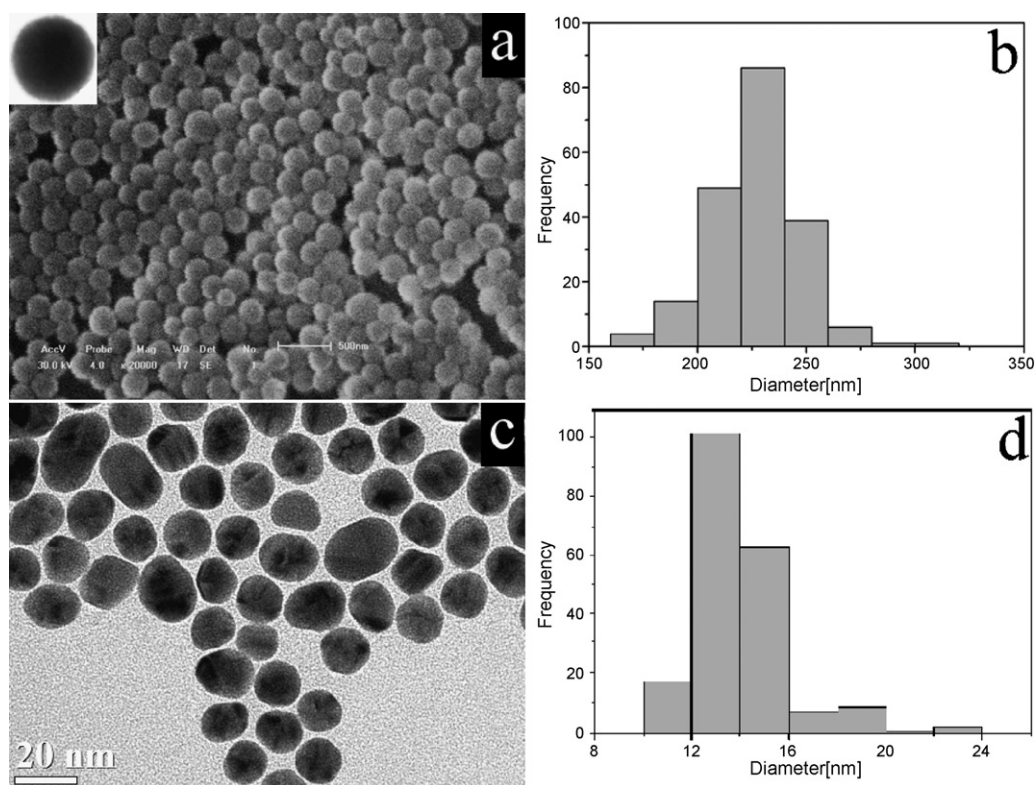


Fig. 4. (a) SEM image of the naked silica microspheres, and the inset is TEM image of a single naked silica microsphere; (b) histogram for the size distribution of silica microspheres; (c) TEM image of Au NPs; (d) histogram for the size distribution of Au NPs.

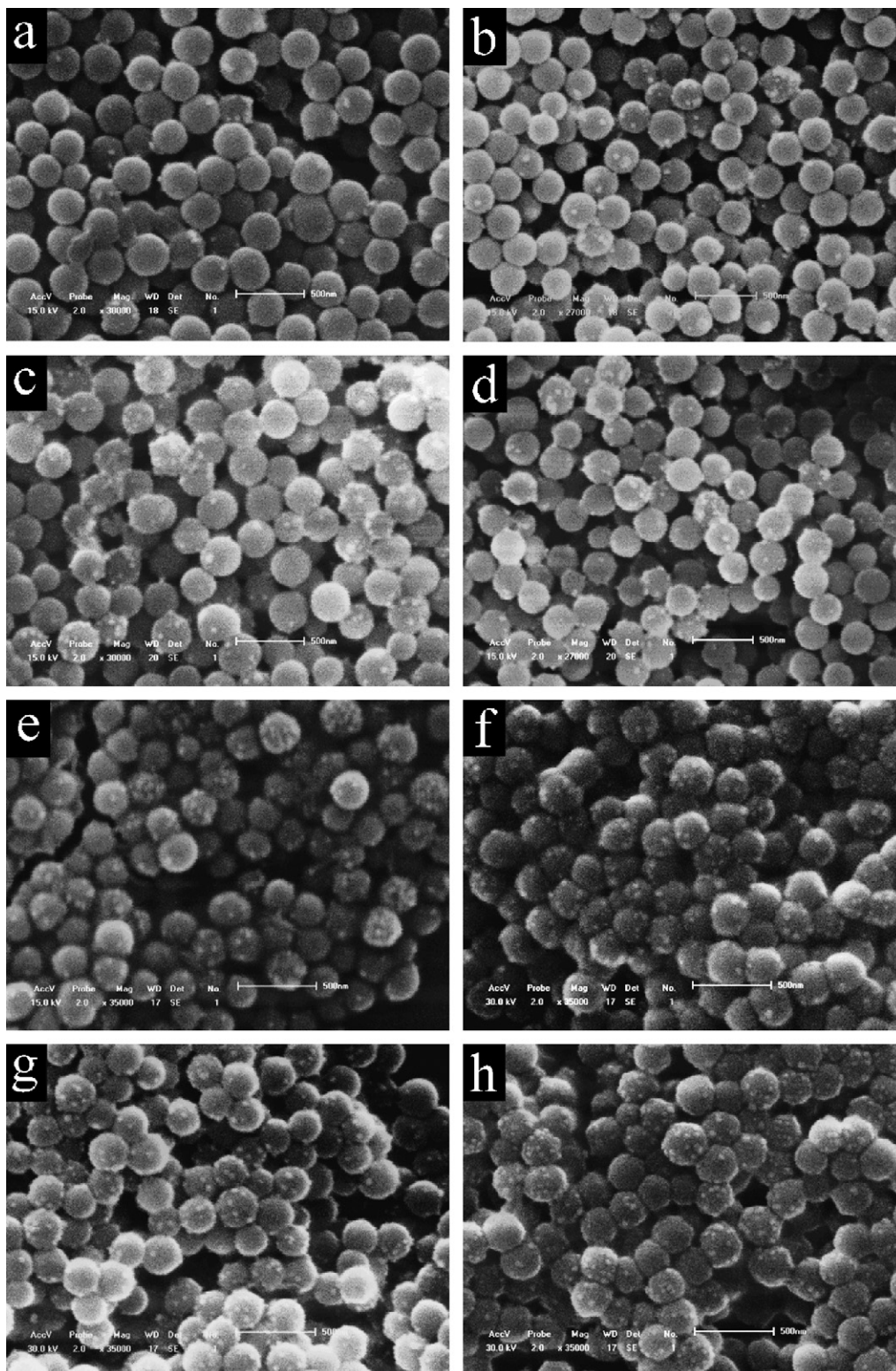


Fig. 5. SEM images of  $\text{SiO}_2@Au$  composite nanoparticles prepared by the first method with various pH values in a wide range: (a) 3.77, (b) 4.65, (c) 5.51, (d) 6.30, (e) 7.79, (f) 9.08, (g) 9.55 and (h) 10.17.

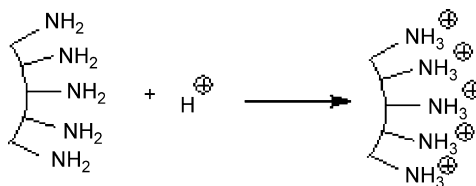


Fig. 6. Schematic procedure of the binding of protons to surface amino groups.

gradually under acidic condition, the Au coverage was decreased correspondingly. Especially when the pH value of the treatment solution fell to around 4, very few Au NPs were attached onto the functionalized silica microspheres. Under basic condition ( $\text{pH} > 7$ ), a denser Au coverage was achieved on silica microspheres (Fig. 5e–h). As the pH values were adjusted to higher levels gradually under basic condition, the Au coverage was increased correspondingly. Obviously, the coverage of Au NPs achieved under basic condition was denser than that under acidic condition. Moreover, the AAS measurement revealed that the sample prepared at 3.77 contained 5.17 wt% Au, while the sample at 10.17 contained 8.84 wt% Au. This result was consistent with the above qualitative analysis.

It indicated that for the three-step method, the  $\text{SiO}_2\text{@Au}$  composite nanoparticles achieved a denser Au coverage on silica microspheres under basic condition than that under acidic condition. Au NPs were attached to surfaces of the functionalized silica microspheres through the coordination bonds between empty orbits of gold atoms and lone-pair electrons of nitrogen atoms. Under acidic condition, most of the amino groups on surfaces of silica microspheres were probably bound with protons so that the Au–N coordinating interaction was broken as shown in Fig. 6.

The UV–vis spectra of the pure Au NPs reduced by sodium citrate exhibited a plasmon absorption peak at 530 nm (Fig. 7a). The absorption peak of the  $\text{SiO}_2\text{@Au}$  nanoparticles obtained at higher pH values had a red shift of about 10 nm (Fig. 7) relative to that of the pure Au NPs. The red shift could be induced by the transfer of most of Au NPs from the solution to surfaces of the functionalized silica microspheres. The absorption peak of  $\text{SiO}_2\text{@Au}$  nanoparticles obtained at lower pH values had little shift relative to that of the pure Au NPs, which was because few Au NPs were attached to surfaces of silica microspheres, and most were still dispersed in the solution. The results of UV–vis spectra were in agreement with the Au coverage shown in the SEM images. In addition, the indented shapes of the absorption peaks were possibly due to the existence of silica microspheres.

### 3.2. $\text{SiO}_2\text{@Au}$ composite nanoparticles II

The  $\text{SiO}_2\text{@Au}$  composite nanoparticles were prepared by the reduction of  $\text{HAuCl}_4$  in the presence of the functionalized silica microspheres. SEM images of the  $\text{SiO}_2\text{@Au}$  nanoparticles illustrated the differences in the

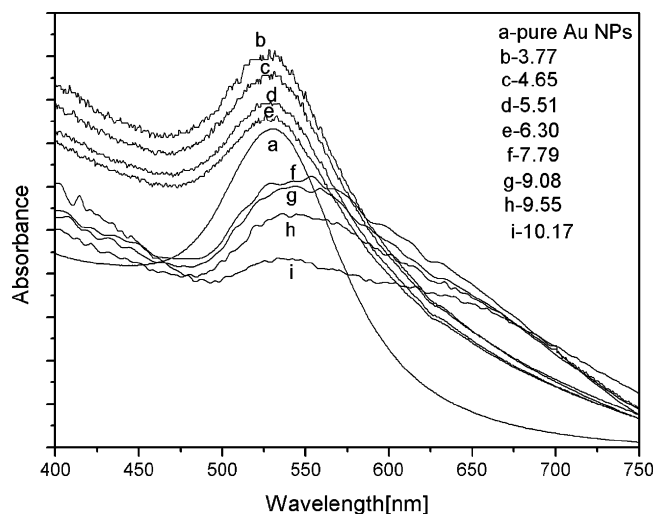


Fig. 7. UV–vis spectra of pure Au NPs (a), and  $\text{SiO}_2\text{@Au}$  composite nanoparticles (b–i) prepared by the first method with various pH values in a wide range.

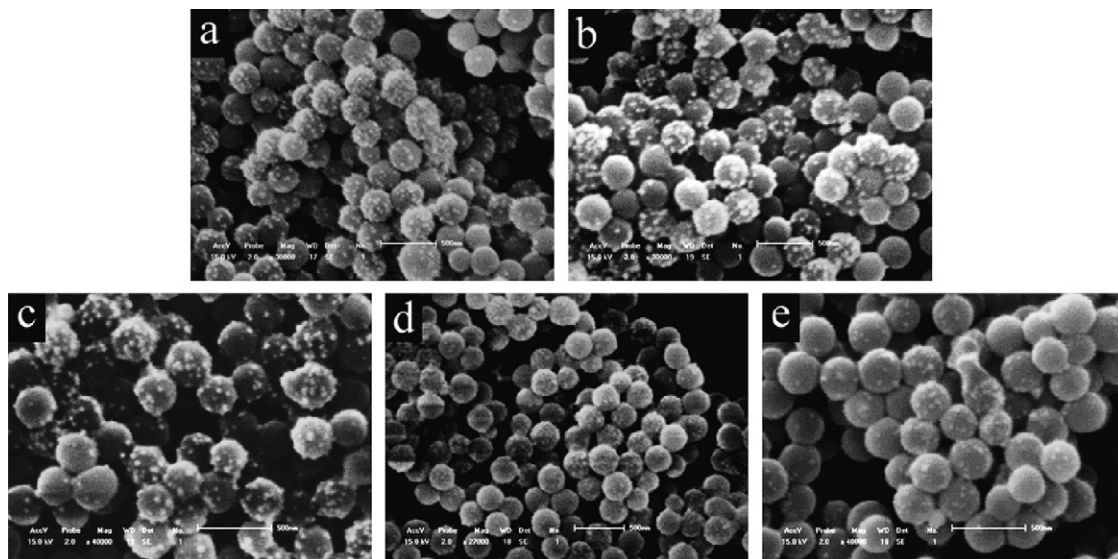


Fig. 8. SEM images of  $\text{SiO}_2\text{@Au}$  composite nanoparticles II prepared at various pH values in a wide range: (a) 3.85, (b) 4.86, (c) 5.38, (d) 7.89 and (e) 8.90.

morphologies of the composite nanoparticles obtained at different pH values. There was an overall trend to the reduction of the Au coverage when the pH values of the treatment solutions were increased gradually (Fig. 8). As the pH value was lowered to around 4, almost each functionalized silica sphere was overlaid with a large amount of Au NPs, forming a dense and uniform Au monolayer (Fig. 8a). The TEM characterization had given us a clearer image that most of the functionalized silica microspheres were covered with a dense Au layer when the pH value was adjusted to 3.85 (Fig. 9). But the amount of the attached Au NPs decreased to a much lower level as the pH value was adjusted to nearly 9 (Fig. 8e). Furthermore, the results of AAS measurement showed us that the higher Au content of 12.65 wt% was gained in the sample at 3.85, and the lower Au content of 10.61 wt% in the sample at 8.90. This result was in agreement with that of SEM observation.

The results revealed that the lower pH values led to a denser Au layer on silica microspheres, while the higher pH values led to a lower Au coverage. Under acidic condition, most of the amino groups on the surfaces of silica microspheres were probably bound with protons originally. However, this binding might be reduced greatly in the following step of heating the mixture of silica microspheres and  $\text{HAuCl}_4$  to reflux. Thus, it was not the major factor for

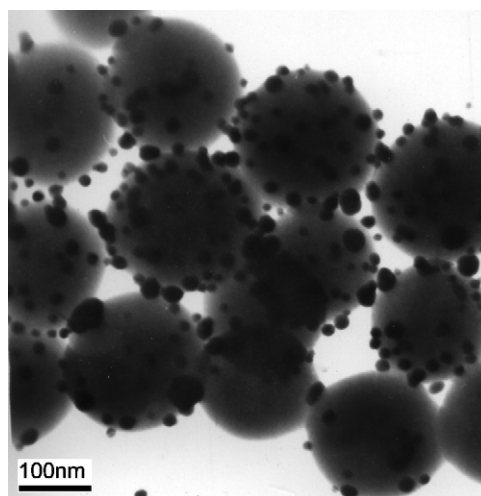


Fig. 9. TEM image of  $\text{SiO}_2\text{@Au}$  composite nanoparticles II at the pH value of 3.85.

the effect of the pH values on the Au coverage any longer. This phenomenon for the pH effect could be accounted for qualitatively by the pH values of the treatment solutions relative to the isoelectric points of silica microspheres and Au NPs. The reported values of the isoelectric point were around 2 for  $\text{SiO}_2$ , and about 6 for Au NPs [32,33]. It indicated that the silica surfaces were negatively charged, respectively, at pH 3.85, 4.86 and 5.38, while Au NPs synthesized by citrate reduction had a positive surface charge. Apparently, Au NPs experienced a significant electrostatic attraction to the silica surfaces with negative charge. Thus, most of Au NPs were deposited by this electrostatic attraction on silica microspheres as soon as they were formed. As the pH value of the treatment solution was increased over 7, the electrostatic attraction referred above was remarkably lowered. Furthermore, the reduction of  $\text{AuCl}_4^-$  ions to Au NPs could not be carried out completely at higher pH values ( $\text{pH} > 7$ ). As a result, a relatively smaller amount of Au NPs were attached.

The UV–vis spectra of  $\text{SiO}_2@$ Au composite nanoparticles prepared using the simplified method were shown in Fig. 10. The spectra of the results obtained at lower pH values all exhibited a plasmon absorption peak at 538 nm (Fig. 10a–c), having a red shift relative to that of the pure Au NPs (Fig. 7a). It could be due to the transfer of most of Au NPs from the solution to the surfaces of the functionalized silica microspheres. The spectra of the results obtained at higher pH values exhibited a plasmon absorption peak at 529 nm, having no distinct shift. The reason could be that few Au NPs were attached to the surfaces of the functionalized silica microspheres.

### 3.3. $\text{SiO}_2@$ Au composite nanoparticles III

In this method, the  $\text{SiO}_2@$ Au composite nanoparticles, prepared by simple mixing Au NPs with the functionalized silica microspheres at room temperature, were transferred into the aqueous solution of  $\text{HAuCl}_4$ , and the mixture was heated to react with a certain reductant. The final products achieved an evidently denser Au coverage than the original  $\text{SiO}_2@$ Au composite nanoparticles prepared at room temperature, as shown in Fig. 11. Moreover, the TEM image (Fig. 12) obviously revealed that the  $\text{SiO}_2@$ Au composite nanoparticles prepared using formaldehyde as the reductant achieved a denser Au layer on the functionalized silica microspheres.

In this method, three reductants had been used: sodium citrate, formaldehyde and sodium hypophosphite. The  $\text{SiO}_2@$ Au composite nanoparticles prepared at room temperature had a low Au coverage (Fig. 11a). The Au coverage was improved as the further reduction of  $\text{AuCl}_4^-$  ions was carried out with any of the three reductants (Fig. 11b–d). The improvement of the Au coverage was partly supported as the Au content was measured for 15.71 wt% in the sample using formaldehyde as the reductant, which was apparently higher than that in the sample prepared by the three-step method.

There could be two possible reasons for the attachment of Au NPs to the surfaces of silica microspheres. The major reason was based on the seeded growth. The whole reaction consisted of two parts. In the first part where the three-step

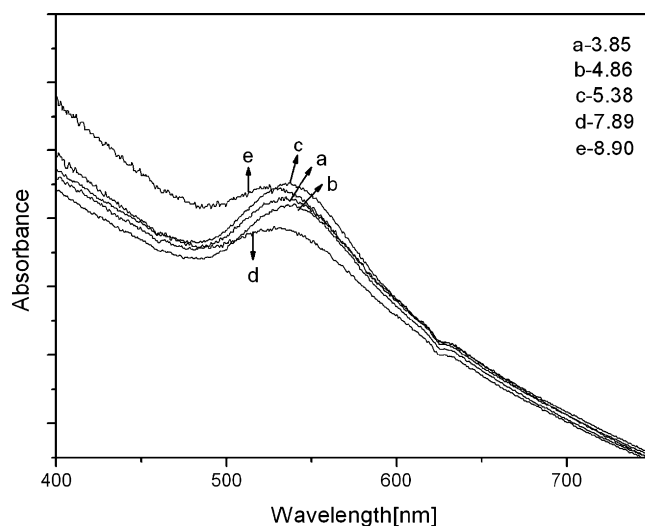


Fig. 10. UV–vis spectra of  $\text{SiO}_2@$ Au composite nanoparticles prepared by the simplified method with various pH values in a wide range.

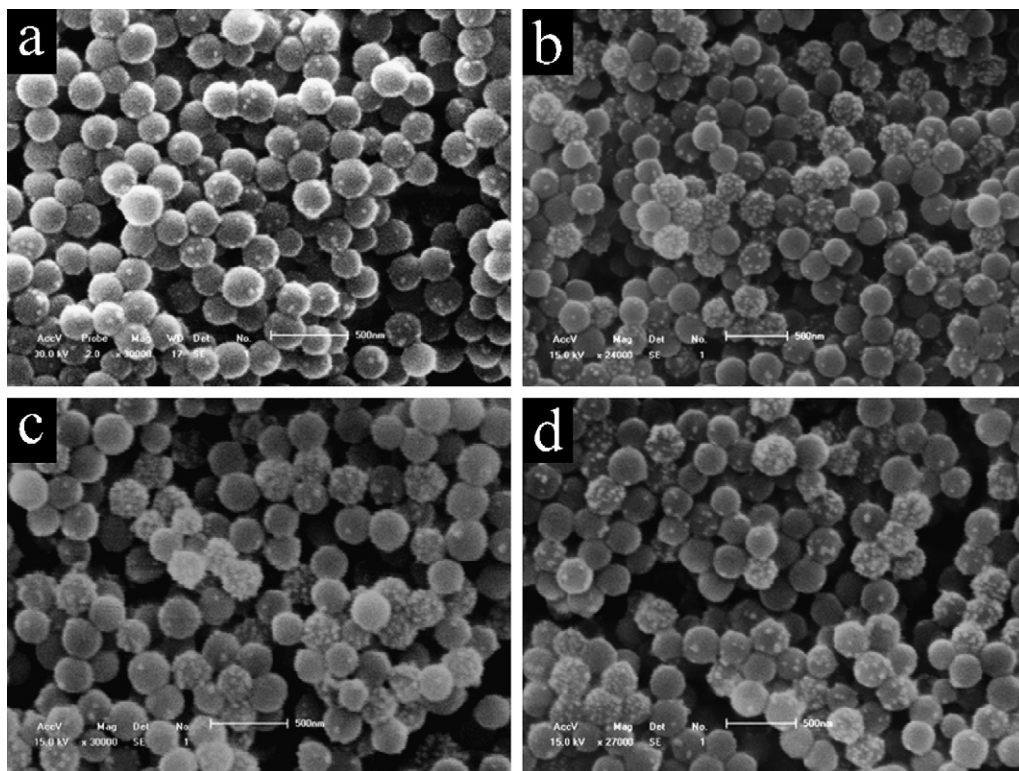


Fig. 11. SEM images of SiO<sub>2</sub>@Au composite nanoparticles prepared using various reductants: (a) SiO<sub>2</sub>@Au, (b) sodium citrate, (c) formaldehyde and (d) sodium hypophosphite.

method was used, Au NPs were tethered on the functionalized silica microspheres by virtue of the aminophilic nature of Au NPs. In the second part where the simplified method was used, the pre-attached Au NPs were used as seeds immobilized on silica microspheres, which provided more nucleation sites for the growth of an Au layer. Obviously, these growing seeds played a role as the link between the silica cores and the freshly formed Au NPs during this

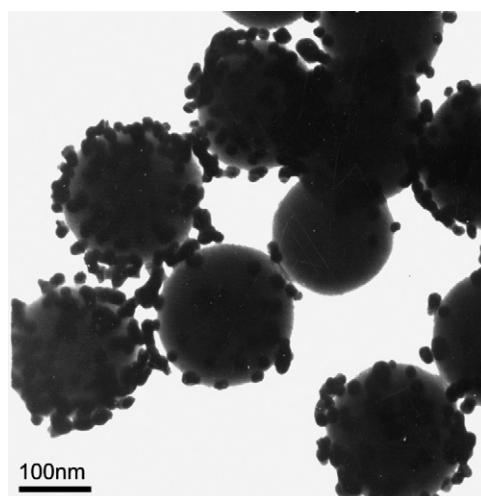


Fig. 12. TEM images of SiO<sub>2</sub>@Au composite nanoparticles prepared by reduction of AuCl<sub>4</sub><sup>-</sup> ions at the boiling point in the presence of the previous SiO<sub>2</sub>@Au synthesized at room temperature.

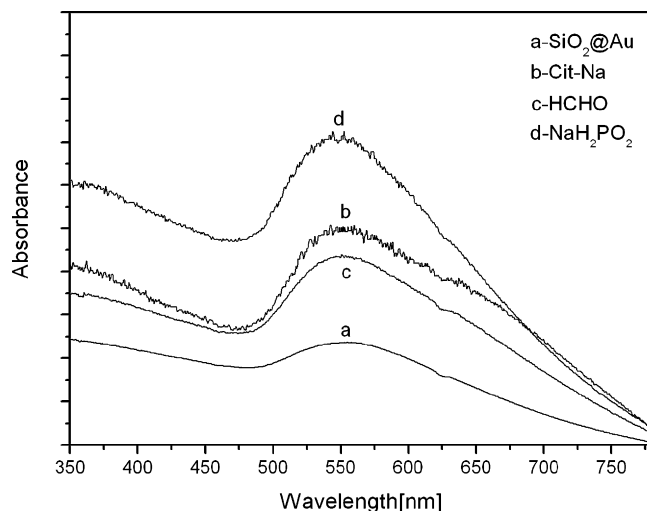


Fig. 13. UV-vis spectra of SiO<sub>2</sub>@Au composite nanoparticles prepared using various reductants.

process. The theory of the seeded growth was also adopted in other people's work [29,34], which mainly introduced the coating of metal nanoparticles on silica microspheres. Another possible reason was the formation of the hydrogen bonds. In the first part of the reaction, the hydrogen bonds could be formed in the solution, which consumed many amino groups on silica microspheres and caused a low coverage of Au NPs. But in the second part, the hydrogen bonds had the possibility to be broken under the higher temperature (100 °C). Thus, the consumed amino groups could be reformed on silica microspheres, which could be coupled with freshly formed Au NPs. The final Au coverage on silica microspheres was enhanced.

The prepared SiO<sub>2</sub>@Au composite nanoparticles using various reductants exhibited the plasmon absorption peaks at 551 nm for sodium citrate (Fig. 13b), 551 nm for formaldehyde (Fig. 13c) and 548 nm for sodium hypophosphite (Fig. 13d). They all had a little red shift compared with the absorption peak of the SiO<sub>2</sub>@Au composite nanoparticles prepared at room temperature (Fig. 13a). It could be caused by the increase of the Au coverage after further reduction of HAuCl<sub>4</sub>.

The results in this case did not give obvious differences among the effects of various reductants on the Au coverage on silica microspheres. But much difference can be found among the three reductants in other aspects. Formaldehyde, a kind of volatile poisonous gas, has much stronger stimulation for human bodies compared with the other two reductants. So the use of formaldehyde may cause the environmental pollution and harm physical health. However, the commercial prices of sodium citrate and sodium hypophosphite are much higher than that of formaldehyde, the use of formaldehyde could lower the cost much.

#### 4. Conclusions

In this paper, we used a simplified method to prepare SiO<sub>2</sub>@Au composite nanoparticles, and compared it with the general three-step method. The results indicated that the simplified method achieved a denser Au layer on silica microspheres. We also made a detailed study on the effect of the pH values on the deposition of Au NPs in both methods. For the three-step method, the lower pH values were unfavorable to the deposition of Au NPs onto silica microspheres; for the simplified method, the higher pH values largely decreased the final Au coverage on silica microspheres.

#### Acknowledgments

This research work was financially supported by the Scientific Research Foundation for the Returned Overseas Chinese Scholars, Ministry of Education, PR China, and the National Natural Science Foundation of China (No. 20473024).

## Appendix A. Supplementary data

Supplementary data associated with this article can be found, in the online version, at [10.1016/j.materresbull.2006.11.019](https://doi.org/10.1016/j.materresbull.2006.11.019).

## References

- [1] G. Schmid, U. Simon, *Chem. Commun.* (2005) 697.
- [2] H.H. Huang, F.Q. Yan, Y.M. Kek, C.H. Chew, G.Q. Xu, W. Ji, P.S. Oh, S.H. Tang, *Langmuir* 13 (1997) 172.
- [3] K.L. Kelly, E. Coronado, L.L. Zhao, G.C. Schatz, *J. Phys. Chem. B* 107 (2003) 668.
- [4] T. Sawitowski, Y. Miquel, A. Heilmann, G. Schmid, *Adv. Funct. Mater.* 11 (2001) 435.
- [5] T. Lutz, C. Estournes, J.L. Guille, *J. Sol–Gel Sci. Technol.* 13 (1998) 929.
- [6] Y.L. Hou, S. Gao, *J. Mater. Chem.* 13 (2003) 1510.
- [7] Z.J. Jiang, C.Y. Liu, L.W. Sun, *J. Phys. Chem. B* 109 (2005) 1730.
- [8] A. Miyazaki, I. Balint, Y. Nakano, *J. Nanopart. Res.* 5 (2003) 69.
- [9] Y. Liu, Y. Chu, L.K. Yang, D.X. Han, Z.X. Lu, *Mater. Res. Bull.* 40 (2005) 1796.
- [10] T. Gao, G.W. Meng, Y.W. Wang, S.H. Sun, L. Zhang, *J. Phys. Condens. Matter* 14 (2002) 355.
- [11] X.C. Wu, Y.R. Tao, *Mater. Res. Bull.* 37 (2002) 2179.
- [12] F. Kim, J.H. Song, P.D. Yang, *J. Am. Chem. Soc.* 124 (2002) 14316.
- [13] N. Cordente, M. Respaud, F. Senocq, M.J. Casanove, C. Amiens, B. Chaudret, *Nano Lett.* 1 (2001) 565.
- [14] J.W. Wang, Y.D. Li, *Adv. Mater.* 15 (2003) 445.
- [15] P. Kohli, J.E. Wharton, O. Braide, C.R. Martin, *J. Nanosci. Nanotechnol.* 4 (2004) 605.
- [16] S.H. Zhang, Z.X. Xie, Z.Y. Jiang, X. Xu, J. Xiang, R.B. Huang, L.S. Zheng, *Chem. Commun.* (2004) 1106.
- [17] S.S. Shankar, S. Bhargava, M. Sastry, *J. Nanosci. Nanotechnol.* 5 (2005) 1721.
- [18] B. Zhang, X.C. Ye, W. Dai, W.Y. Hou, F. Zuo, Y. Xie, *Nanotechnology* 17 (2006) 385.
- [19] Y. Kobayashi, V. Salgueirino-Maceira, L.M. Liz-Marzan, *Chem. Mater.* 13 (2001) 1630.
- [20] V.G. Pol, A. Gedanken, J. Calderon-Moreno, *Chem. Mater.* 15 (2003) 1111.
- [21] J. Gao, F.Q. Tang, J. Ren, *Surf. Coat. Technol.* 200 (2005) 2249.
- [22] H.L. Xia, F.Q. Tang, *J. Phys. Chem. B* 107 (2003) 9175.
- [23] S. Chakrabarti, S.K. Mandal, B.K. Nath, D. Das, D. Ganguli, S. Chaudhuri, *Eur. Phys. J. B* 34 (2003) 163.
- [24] H.J. Dun, W.Q. Zhang, Y. Wei, X.Q. Song, Y.M. Li, L.R. Chen, *Anal. Chem.* 76 (2004) 5016.
- [25] N.A. Dhas, A. Zaban, A. Gedanken, *Chem. Mater.* 11 (1999) 806.
- [26] N.A. Dhas, A. Gedanken, *Appl. Phys. Lett.* 72 (1998) 2514.
- [27] S.L. Westcott, S.J. Oldenburg, T.R. Lee, N.J. Halas, *Langmuir* 14 (1998) 5396.
- [28] Y. Kobayashi, Y. Tadaki, D. Nagao, M. Konno, *J. Colloid Interface Sci.* 283 (2005) 601.
- [29] Y.T. Lim, O.O. Park, H.T. Jung, *J. Colloid Interface Sci.* 263 (2003) 449.
- [30] W. Wang, C.M. Ruan, B.H. Gu, *Anal. Chim. Acta* 567 (2006) 121.
- [31] W. Stober, A. Fink, *J. Colloid Interface Sci.* 26 (1968) 62.
- [32] I. Hussain, M. Brust, A.J. Papworth, A.I. Cooper, *Langmuir* 19 (2003) 4831.
- [33] J.G. Yu, H.G. Yu, B. Cheng, X.J. Zhao, J.C. Yu, W.K. Ho, *J. Phys. Chem. B* 107 (2003) 13871.
- [34] Z.J. Jiang, C.Y. Liu, *J. Phys. Chem. B* 107 (2003) 12411.